




# CXCL10/CXCR3 Signaling in the DRG Exacerbates Neuropathic Pain in Mice

Yan-Fang Kong<sup>1</sup> · Wei-Lin Sha<sup>1</sup> · Xiao-Bo Wu<sup>1</sup> · Lin-Xia Zhao<sup>1</sup> · Ling-Jie Ma<sup>1</sup> · Yong-Jing Gao<sup>1,2</sup> 

Received: 21 February 2020 / Accepted: 22 June 2020 / Published online: 16 November 2020  
© Shanghai Institutes for Biological Sciences, CAS 2020

**Abstract** Chemokines and receptors have been implicated in the pathogenesis of chronic pain. Here, we report that spinal nerve ligation (SNL) increased CXCR3 expression in dorsal root ganglion (DRG) neurons, and intra-DRG injection of *Cxcr3* shRNA attenuated the SNL-induced mechanical allodynia and heat hyperalgesia. SNL also increased the mRNA levels of CXCL9, CXCL10, and CXCL11, whereas only CXCL10 increased the number of action potentials (APs) in DRG neurons. Furthermore, in *Cxcr3*<sup>-/-</sup> mice, CXCL10 did not increase the number of APs, and the SNL-induced increase of the numbers of APs in DRG neurons was reduced. Finally, CXCL10 induced the activation of p38 and ERK in ND7-23 neuronal cells and DRG neurons. Pretreatment of DRG neurons with the P38 inhibitor SB203580 decreased the number of APs induced by CXCL10. Our data indicate that CXCR3, activated by CXCL10, mediates p38 and ERK activation in DRG neurons and enhances neuronal excitability, which contributes to the maintenance of neuropathic pain.

**Keywords** CXCR3 · CXCL10 · DRG · Neuropathic pain · Mice

## Introduction

Neuropathic pain is caused by disease or injury of the sensory nervous system and affects up to 8% of the population [1]. However, the mechanisms underlying neuropathic pain remains elusive. Accumulating evidence supports the idea that chemokine-mediated neuroinflammation plays an important role in the development and maintenance of neuropathic pain [2–4]. Several chemokines, such as CX3CL1, CCL2, CXCL1, CXCL13, and CXCL10 are increased in the spinal cord after tissue inflammation or nerve injury and contribute to inflammatory pain and neuropathic pain *via* different forms of neuron–glial interaction [5–9]. However, the roles and mechanisms of chemokines and chemokine receptors in the dorsal root ganglion (DRG) in mediating chronic pain have been less investigated.

CXC chemokine receptor 3 (CXCR3), the receptor of the three ligands CXCL9, CXCL10, and CXCL11, is expressed in various cells, including endothelial cells, monocytes, T cells, and dendritic cells [10]. The activation of CXCR3 by its ligands contributes to the progression of autoimmune diseases and infections [10, 11]. Recent studies have shown that CXCR3 is expressed in spinal neurons and is increased after spinal nerve ligation (SNL) [7] or inoculation of cancer cells into the tibia [12]. SNL also increases the expression of CXCL9, CXCL10, and CXCL11 in spinal astrocytes [7, 13]. Perfusion of neurons in lamina II of the dorsal horn with CXCL10 enhances excitatory synaptic transmission *via* neuronal CXCR3, whereas CXCL9 and CXCL11 increase both the excitatory and inhibitory synaptic transmission of lamina II neurons [7, 13]. Previous studies have implied that the three ligands of CXCR3 have different temporal and spatial patterns of expression, and are regulated by different stimuli during

Yan-Fang Kong and Wei-Lin Sha have contributed equally to this work.

✉ Yong-Jing Gao  
gaoyongjing@ntu.edu.cn; gaoyongjing@hotmail.com

<sup>1</sup> Institute of Pain Medicine, Institute of Nautical Medicine, Nantong University, Nantong 226019, China

<sup>2</sup> Co-Innovation Center of Neuroregeneration, Nantong University, Nantong 226001, China

the course of the immune response [14, 15]. How CXCR3 and its ligands are regulated in the DRG after SNL and whether they are involved in neuropathic pain remain unknown.

Peripheral nerve injury is associated with changes in the excitability of sensory neurons in the DRG [16]. Several chemokines are expressed in the DRG and contribute to the regulation of neuronal excitability [16]. For example, CCL2 increases Na<sup>+</sup> currents in DRG neurons [17]; CXCL1 enhances the excitability of DRG neurons by regulating Na<sup>+</sup> and K<sup>+</sup> currents [18, 19]; CXCL13 is increased in DRG neurons after SNL as does Nav1.8 current density [20]. Whether the ligands of CXCR3 regulate the neuronal excitability of DRG neurons is of interest.

Chemokine receptors belong to the 7-transmembrane G-protein-coupled receptors, which can activate intracellular kinases, including mitogen-activated protein kinases (MAPKs) [4]. Members of the MAPK family, including extracellular signal-regulated kinase (ERK), p38, and c-Jun N-terminal kinase (JNK), are activated in the spinal cord by peripheral nerve injury [21]. ERK and p38 are also expressed and increased in the DRG under chronic pain conditions [22]. In addition, activated ERK increases the expression of the Na<sup>+</sup> channel Nav1.8 or phosphorylates Nav1.7 and alters its gating properties [23, 24], while activated p38 directly regulates the phosphorylation of Nav1.8 in DRG neurons [25]. Our previous data showed that intrathecal injection of CXCL10 induces rapid ERK activation in the spinal cord [7]. Thus, we hypothesized that CXCR3 can be activated by CXCL10 and further enhances MAPK-dependent neuronal excitability and exacerbates neuropathic pain after SNL. To test the hypothesis, we examined the mRNA and protein expression of CXCR3 in the DRG after SNL. We further investigated the direct role of CXCR3 ligands on regulating neuronal excitability in DRG neurons. Our results demonstrated that CXCR3 is activated by CXCL10 and enhances neuronal excitability *via* p38 MAPK and contributes to the maintenance of neuropathic pain.

## Materials and Methods

### Animals and Surgery

ICR mice and C57BL/6 mice (6–8 weeks old, male) were purchased from the Experimental Animal Center of Nantong University. *Cxcr3*<sup>-/-</sup> mice were purchased from the Jackson Laboratory (stock No. 005796). All mice had free access to food and water. The animal facility was maintained at 23°C ± 1°C on a 12:12 h light-dark cycle. All experimental procedures were approved by the Animal

Care and Use Committee of Nantong University. Animal treatments were performed in accordance with the guidelines of International Association for the Study of Pain. For the SNL surgery, we isolated the left L5 spinal nerve and tightly ligated it with 6–0 silk suture. In sham-operated animals, the same procedure was performed except for ligation.

### Drugs and Administration

Recombinant CXCL10 (murine) was from PeproTech (Rocky Hills, NJ, USA) and the p38 MAPK inhibitor SB203580 was from Tocris (Bristol, UK). For intrathecal injection, the animals were anesthetized with isoflurane, and the reagents were injected into the subarachnoid space through a 30G needle.

### Real-Time Quantitative PCR

The total RNA of the DRG was extracted using TRIzol reagent (Invitrogen, Carlsbad, CA, USA) as described previously [26]. Quantitative polymerase chain reaction (qPCR) analysis was performed in a real-time detection system (RotorGene 6000, Qiagen) by SYBR green I dye detection (Takara, Japan). The following primers were used: *Cxcr3* forward, 5'-TAC CTT GAG GTT AGT GAA CGT CA-3'; *Cxcr3* reverse, 5'-CGC TCT CGT TTT CCC CAT AAT C-3'; *Cxcl9* forward, 5'-GGA GTT CGA GGA ACC CTA GTG-3'; *Cxcl9* reverse, 5'-GGG ATT TGT AGT GGA TCG TGC-3'; *Cxcl10* forward, 5'-TGA ATC CGG AAT CTA AGA CCA TCA A-3'; *Cxcl10* reverse, 5'-AGG ACT AGC CAT CCA CTG GGT AAA G-3'; *Cxcl11* forward, 5'-GGC TTC CTT ATG TTC AAA CAG GG-3'; *Cxcl11* reverse, 5'-GCC GTT ACT CGG GTA AAT TAC A-3'; *Gapdh* forward, 5'-AAA TGG TGA AGG TCG GTG TGA AC-3'; and *Gapdh* reverse, 5'-CAA CAA TCT CCA CTT TGC CAC TG-3'. PCR amplification was performed at 95°C for 3 min followed by 40 cycles of cycling at 95°C for 10 s and 60°C for 30 s. *Gapdh* was used as an internal control for normalization. The ratios of mRNA levels were calculated using the  $-\Delta\Delta C_t$  method ( $2^{-\Delta\Delta C_t}$ ).

### Immunohistochemistry

For immunofluorescence staining, mice were deeply anesthetized and transcardially perfused with 4% paraformaldehyde. DRG sections were cut at 15 μm on a cryostat and processed for immunostaining as previously described [27]. The following primary antibodies were used: CXCR3 (rabbit, 1:200, Boster Biological Technology, Wuhan, China), CXCL10 (goat, 1:100, R&D Systems, Minneapolis, MN, USA), β3-tubulin (mouse, 1:500, R&D Systems), IBA-1 (goat, 1:1000, Abcam, Cambridge, MA,

USA and rabbit, 1:3000, Wako, Japan), and GFAP (mouse, 1:5000, Millipore, Billerica, MA, USA). The sections were then incubated with Cy3- or Alexa 488-conjugated secondary antibodies (1:1000, Jackson, West Grove, PA, USA). A Leica SP8 confocal microscope was used to examine the stained sections and capture images.

### ND7/23 Cell Culture

ND7/23 cells were maintained in high-glucose Dulbecco's modified Eagle's medium (DMEM, Corning, USA) supplemented with 10% fetal bovine serum and 1% penicillin-streptomycin. The cells were plated in 12-well plates under 5% CO<sub>2</sub> and 95% O<sub>2</sub> at 37°C. Experiments were performed when the cells had grown to 90% confluence. Prior to stimulation with CXCL10 (10 ng/mL), high glucose DMEM was replaced with Opti-MEM (Corning, USA). Cells were incubated with CXCL10 for 30 min, 60 min, 3 h, or 6 h depending on the experiment. After treatment, the cells were collected for Western blot.

### Western Blot

The DRG tissue and cells were homogenized in a lysis buffer containing protease and phosphatase inhibitors (Sigma, St. Louis, MO, USA). The BCA Protein Assay was used to determine the protein concentrations. SDS-PAGE and western blot were performed as previously described [27]. The following antibodies were used: pp38 (rabbit, 1:1000, Cell Signaling, Boston, MA, USA), p38 (rabbit, 1:1000, Cell Signaling), pERK (rabbit, 1:1000, Cell Signaling), ERK (rabbit, 1:1000, Cell Signaling), and IRDye 800CW secondary antibody. The images were captured by an Odyssey Imaging System (LI-COR Bioscience, Lincoln, NE, USA).

### Lentiviral Vector Production and DRG Microinjection

shRNAs targeting the sequence of mouse *Cxcr3* (5'-CTG AAC TTT GAC AGA ACC T-3'. Gene Bank Accession: NM\_009910.2) and a scrambled sequence (5'-TTC TCC GAA CGT GTC ACG T-3', negative control, NC) were designed. Recombinant lentivirus containing *Cxcr3* shRNA (LV-*Cxcr3* shRNA) or NC shRNA (LV-NC) was packaged using the pGCSIL-GFP vector by Shanghai GeneChem. The knockdown effect of the *Cxcr3* shRNA had been tested in our previous study [26]. Before the DRG microinjection, we exposed the unilateral L5 DRG. The LV-*Cxcr3* shRNA (2 µL) was injected into the DRG through a glass micropipette. The same volume of LV-NC shRNA was used as a control. The glass micropipette was removed 10 min after administration.

### Behavioral Testing

Mice were habituated to the testing environment daily for 2 days before experiments. For mechanical allodynia, the mice were put in metal mesh boxes and allowed ~1 h for habituation. The paw withdrawal threshold was measured according to the logarithmically incremental stiffness of von Frey filaments (0.02 g, 0.04 g, 0.07 g, 0.16 g, 0.40 g, 0.60 g, 1.0 g, and 2.0 g) with an up-down method to assess tactile allodynia [28]. To test heat hyperalgesia, the mice were put in a plastic box placed on a glass plate. A beam of radiant heat was applied to the plantar surface through the transparent glass surface [29] and the paw withdrawal latency was recorded. The baseline latency was adjusted to 10 s–15 s, and 20 s was used as the cutoff to prevent potential injury.

### Preparation of DRG Neurons and Electrophysiological Recording

DRG neurons from mice 4–6 weeks old were dissociated and cultured as described previously [20]. In brief, the mice were deeply anesthetized by exposure to isoflurane. Lumbar DRGs (L4–L6) were quickly excised and placed in ice-cold oxygenated artificial cerebrospinal fluid (ACSF) [27]. After removing the connective tissue, the ganglia were transferred to a dissecting solution containing collagenase D and trypsin, and then washed and transferred into normal oxygenated ACSF at room temperature for recording.

The electrophysiological recording was performed as previously described [20]. In brief, neurons were visualized under an upright infrared-differential interference contrast microscope (BX51WI, Olympus). The patch pipettes were pulled from borosilicate glass capillaries using a P-97 Flaming micropipette puller (Sutter Instruments). The initial resistance was 4 MΩ–8 MΩ when filled with the internal solution. A Multiclamp 700B amplifier (Molecular Devices) was used for the whole-cell patch-clamp recording. Signals were acquired and analyzed with pClamp 10 software (Axon Instruments).

We chose neurons with diameters < 25 µm for recording. Membrane potential was measured with a pipette solution containing (in mmol/L): 120 potassium gluconate, 2 MgCl<sub>2</sub>, 0.3 EGTA, 10 HEPES, 20 KCl, and 4 Na<sub>2</sub>ATP. To study the excitability of neurons, the resting potential (RP) and action potentials (APs) were recorded. APs were evoked by a series of ramp currents (Current intensity, 100 pA–300 pA; duration, 1 s).

For drug treatment, the ganglia were incubated with CXCL9, CXCL10, or CXCL11 for 30 min before recording. The P38 inhibitor SB203580 was incubated for 30 min

before co-treatment with CXCL10. Experimental data were analyzed using Clampfit (version 8.0; OriginLab).

### Quantification and Statistics

GraphPad Prism v5.0 was used for statistical analyses. All of the results are presented as mean  $\pm$  SEM. The behavioral data were analyzed by two-way repeated measures (RM) ANOVA followed by the Bonferroni test. The qPCR data were analyzed by one-way ANOVA followed by the Bonferroni test. For western blot, the density of specific bands was measured with ImageJ (NIH,

Bethesda, MD, USA). Differences between two groups were compared using Student's *t*-test. For all experiments,  $P < 0.05$  was considered to be significant ( $*P < 0.05$ ,  $**P < 0.01$ ,  $***P < 0.001$ ).

### Results

#### SNL Increases CXCR3 Expression in DRG Neurons

We first used qPCR to check the time-course of *Cxcr3* mRNA expression in the DRG after SNL or sham-

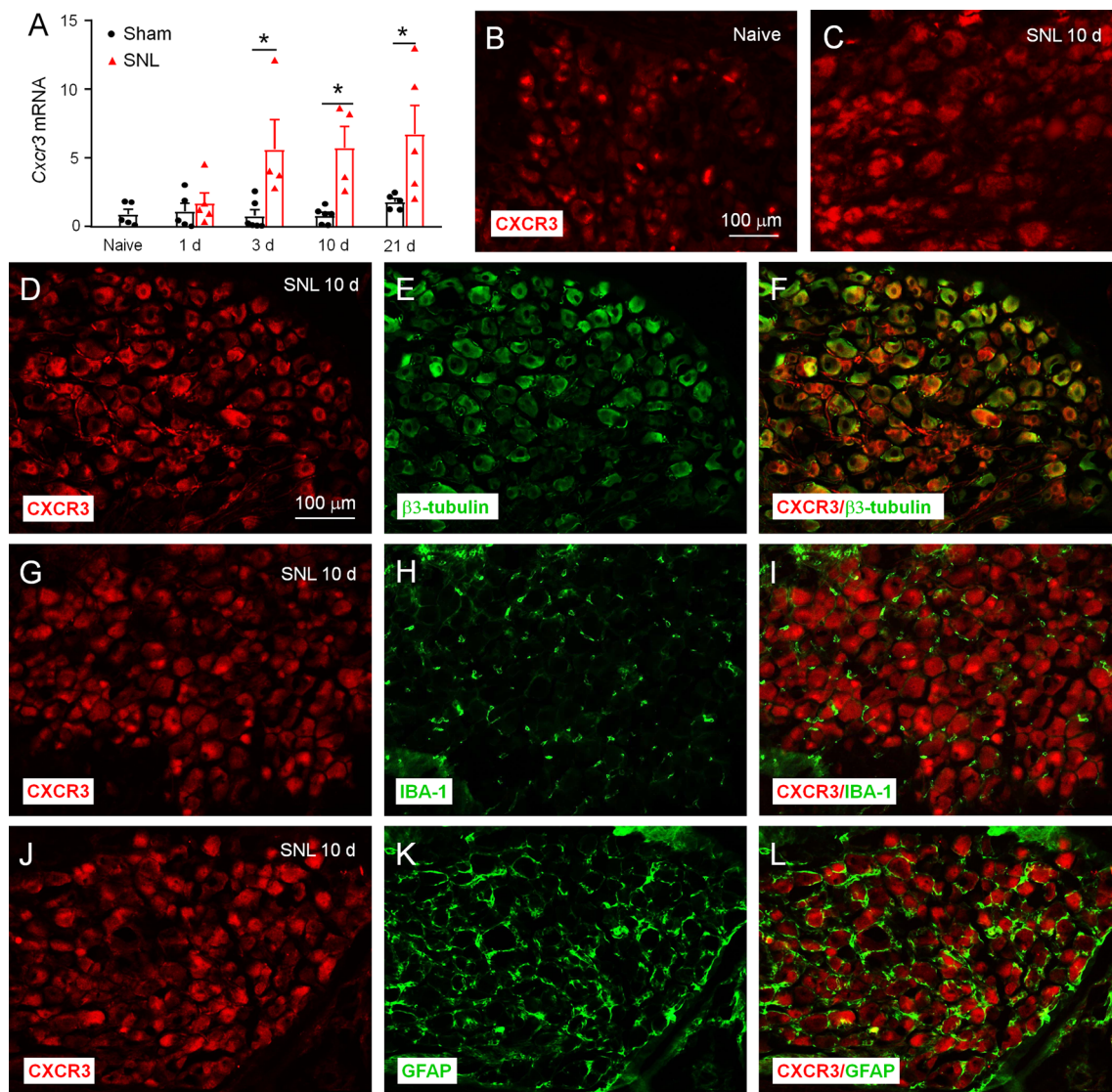


**Fig. 1** SNL increases CXCR3 expression in DRG neurons. **A** Time-course of *Cxcr3* mRNA expression in the DRG from naïve, sham-, and SNL-operated mice. The mRNA expression of *Cxcr3* was increased at days 3, 10, and 21 after SNL.  $n = 4-6$  mice per group.  $*P < 0.05$  vs corresponding sham group; Student's *t*-test. **B, C** Representative images of CXCR3 immunofluorescence in the DRG

from naïve and SNL mice. CXCR3 was constitutively expressed in naïve mice (**B**) and increased in SNL-operated mice (**C**). **D-L** Double immunofluorescence staining showing that CXCR3 mainly colocalized with the neuronal marker  $\beta$ 3-tubulin (**D-F**), but not with the macrophage marker IBA-1 (**G-I**) or the satellite marker GFAP (**J-L**) in the DRG 10 days after SNL.

operation. Compared with sham-operated mice, *Cxcr3* mRNA was significantly increased from 3–21 days after SNL (day 3,  $5.75 \pm 2.16$ -fold,  $P < 0.05$ ; day 10,  $5.84 \pm 1.55$ -fold,  $P < 0.01$ ; day 21,  $6.85 \pm 2.09$ -fold,  $P < 0.05$ ; Student's *t*-test; Fig. 1A). We then checked the CXCR3 distribution in the DRG by immunofluorescence staining. CXCR3-immunoreactivity (IR) was shown in the DRG from naïve mice (Fig. 1B), and a marked increase in CXCR3-IR was induced 10 days after SNL (Fig. 1C). To define the cellular localization of CXCR3 in the DRG, we used double-staining of CXCR3 with the neuronal marker  $\beta$ -tubulin, the macrophage marker IBA-1, and the satellite cell marker GFAP. The results showed that the CXCR3 largely co-localized with  $\beta$ -tubulin (Fig. 1D–F), but not with IBA-1 (Fig. 1G–I) or GFAP (Fig. 1J–L), suggesting neuronal expression of CXCR3 in the DRG.

### Inhibition of CXCR3 Level in the L5 DRG Alleviates SNL-Induced Pain Hypersensitivity

To investigate the role of CXCR3 in the DRG in the pathogenesis of neuropathic pain, we microinjected control lentivirus (LV-NC) and *Cxcr3* shRNA lentivirus (LV-*Cxcr3* shRNA) into the L5 DRG after SNL. Five days after lentivirus injection, GFP was evident in many DRG neurons (Fig. 2A, B). We then compared the *Cxcr3* mRNA level in the DRG of sham, LV-NC-treated, and LV-*Cxcr3*

shRNA-treated SNL mice. qPCR showed that *Cxcr3* mRNA was significantly higher in LV-NC shRNA-injected SNL mice than in sham-operated mice ( $1 \pm 0.31$  vs  $4.53 \pm 0.74$ ,  $P < 0.001$ , one-way ANOVA). In addition, DRG injection of LV-*Cxcr3* shRNA caused a significant reduction of *Cxcr3* mRNA expression compared to LV-NC shRNA injection ( $0.60 \pm 0.28$  vs  $4.53 \pm 0.74$ ,  $P < 0.001$ , one-way ANOVA, Fig. 2C), confirming the knockdown effect of LV-*Cxcr3* shRNA in the L5 DRG. We then checked pain behaviors of the three groups of mice. As shown in Fig. 2D, E, compared to sham, the mice in the SNL+LV-NC group showed dramatic decreases in mechanical allodynia and heat hyperalgesia ( $P < 0.001$ , two-way RM ANOVA followed by the Bonferroni test). Furthermore, LV-*Cxcr3* shRNA markedly attenuated the SNL-induced mechanical allodynia at days 5, 10, and 14 after SNL (Treatment,  $F_{1,59} = 20.48$ ,  $P < 0.0001$ ; Time,  $F_{3,59} = 51.12$ ,  $P < 0.0001$ ; Interaction,  $F_{3,59} = 3.366$ ,  $P < 0.05$ ; two-way RM ANOVA; Fig. 2D). LV-*Cxcr3* shRNA treatment also reversed the SNL-induced heat hyperalgesia at days 5, 10, and 14 (Treatment,  $F_{1,62} = 55.30$ ,  $P < 0.0001$ ; Time,  $F_{3,62} = 77.76$ ,  $P < 0.0001$ ; Interaction,  $F_{3,62} = 10.04$ ,  $P < 0.0001$ ; two-way RM ANOVA; Fig. 2E). Collectively, the results suggest that CXCR3 in the DRG is involved in the pathogenesis of neuropathic pain.

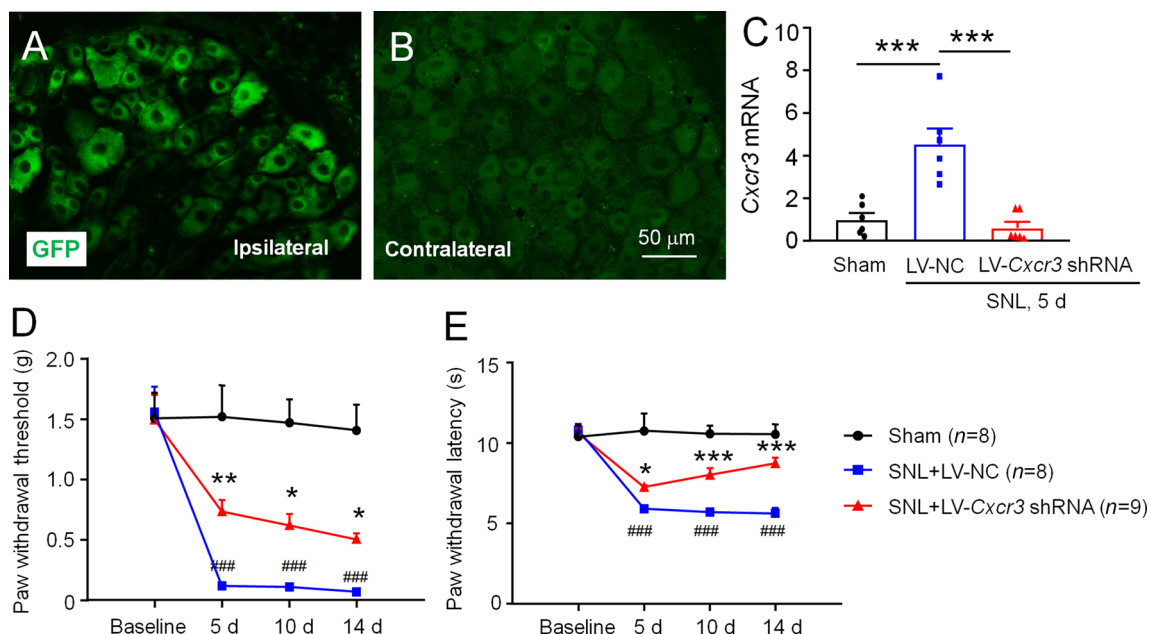


**Fig. 2** Inhibition of CXCR3 in the DRG attenuates neuropathic pain. **A, B** GFP fluorescence in a DRG injected with LV-*Cxcr3* shRNA (**A**), whereas the contralateral DRG has no fluorescence (**B**). **C** The mRNA expression of CXCR3 was increased in the SNL + LV-NC shRNA group, and this was decreased in LV-*Cxcr3* shRNA group ( $n = 6$  mice per group;  $***P < 0.001$ , one-way ANOVA). **D, E** Microinjection of

LV-*Cxcr3* shRNA lentivirus in the DRG after SNL persistently alleviated SNL-induced mechanical allodynia (**D**) and reversed heat hyperalgesia (**E**) ( $n = 8$ – $9$  mice per group;  $*P < 0.05$ ,  $**P < 0.01$ ,  $***P < 0.001$  vs LV-NC group,  $###P < 0.001$  vs sham group; two-way RM ANOVA followed by the Bonferroni test).

### SNL Increases the mRNA Levels of CXCL9, CXCL10, and CXCL11, but Only CXCL10 Increases the Excitability of DRG Neurons

Before checking whether the ligands of CXCR3 can increase neuronal excitability, we briefly examined the mRNA levels of CXCL9, CXCL10, and CXCL11 in the DRG after SNL. QPCR showed that *Cxcl9* mRNA was increased on day 21 after SNL (day 21,  $21.03 \pm 3.99$ -fold,  $P < 0.01$ , SNL vs sham, Student's *t*-test, Fig. 3A). *Cxcl10* mRNA was increased from days 3–21 after SNL (day 3,  $5.61 \pm 1.68$ -fold,  $P < 0.05$ ; day 10,  $16.71 \pm 1.62$ -fold,  $P < 0.001$ ; day 21,  $21.89 \pm 5.51$ -fold,  $P < 0.001$ , SNL vs sham, Student's *t*-test, Fig. 3B). *Cxcl11* mRNA was increased on

days 10 and 21 (day 10,  $2.40 \pm 0.36$ -fold,  $P < 0.01$ ; day 21,  $3.25 \pm 0.30$ -fold,  $P < 0.001$ , SNL vs sham, Student's *t*-test, Fig. 3C). These data suggest that CXCL10 is increased in the early and late phases, whereas CXCL9 and CXCL11 are increased in the late phase.

We then compared the evoked APs in whole-mount DRG neurons incubated with CXCL9, CXCL10, or CXCL11 at 100 ng/mL for 30 min. In responding to 100 pA, 200 pA, and 300 pA ramp currents, the numbers of APs in control (PBS) neurons were  $5.5 \pm 0.43$ ,  $9.5 \pm 0.89$ , and  $12.4 \pm 1.2$ , respectively. After incubation with CXCL9 or CXCL11, the number of APs was not significantly changed (CXCL9 vs PBS: Treatment,  $F_{1,54} = 0.012$ ,  $P > 0.05$ ; CXCL11 vs PBS: Treatment,  $F_{1,56} = 0.2086$ ,  $P >$

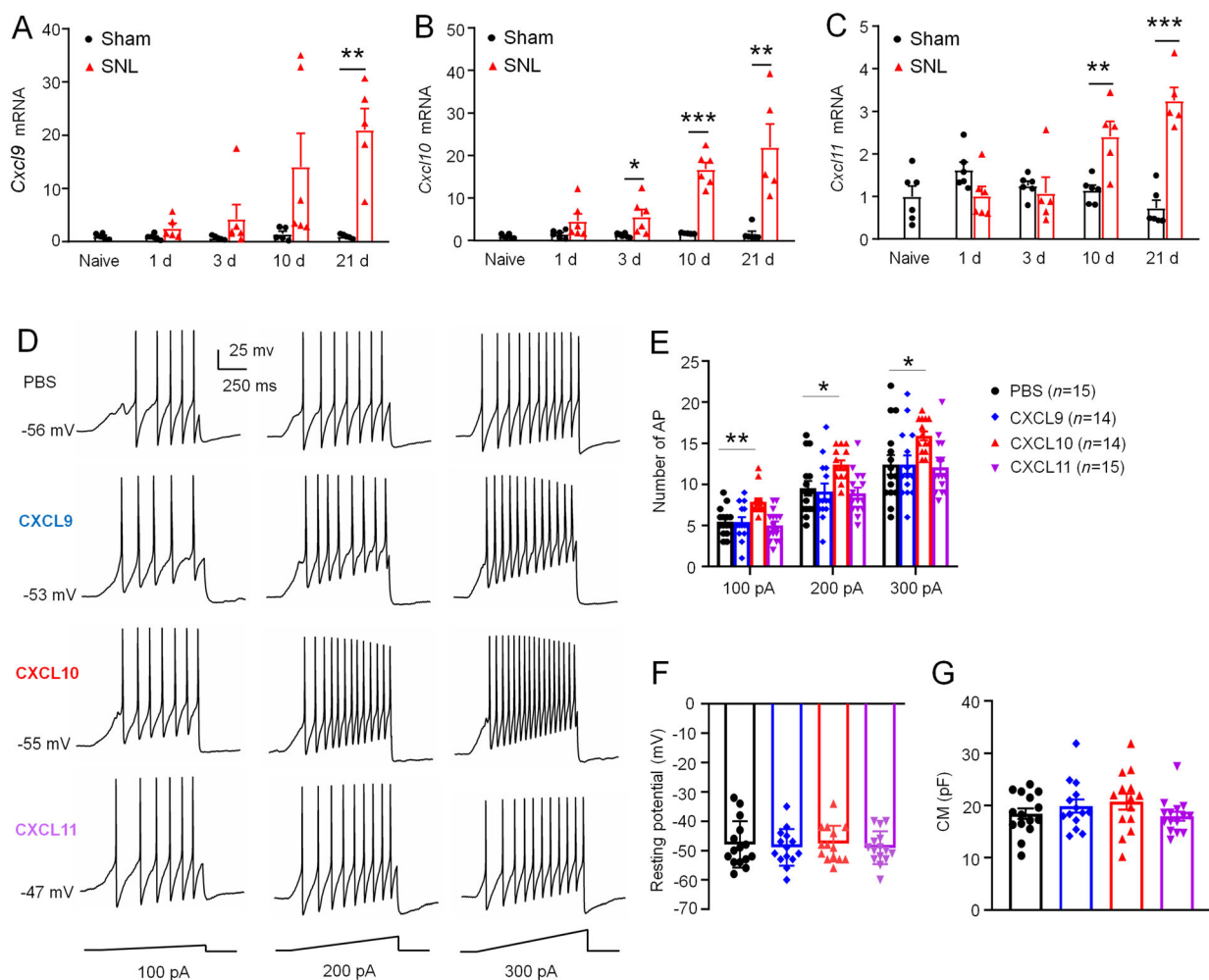


**Fig. 3** CXCL10 increases the excitability of DRG neurons. **A–C** Time-course of *Cxcl9*, *Cxcl10*, and *Cxcl11* mRNA expression in the DRG in naïve, sham-, and SNL-operated mice ( $n = 5–6$  mice per group;  $*P < 0.05$ ,  $**P < 0.01$ ,  $***P < 0.001$  vs corresponding sham group; Student's *t*-test). **D** Examples of membrane potential responses from WT mice evoked by 1000 ms ramp current injection of 100 pA, 200 pA, and 300 pA in neurons incubated with CXCL9, CXCL10, or

CXCL11. **E** Histogram showing the numbers of APs in DRG neurons from CXCL9-, CXCL10-, or CXCL11-incubated WT mice ( $*P < 0.05$ ,  $**P < 0.01$  vs PBS; two-way RM ANOVA followed by Bonferroni test). **F, G** The Resting Potential (**F**) and CM (**G**) after treatment with PBS, CXCL9, CXCL10, or CXCL11. There were no differences between these groups.

0.05, two-way ANOVA, Fig. 3D). However, the number of APs was significantly increased in DRG neurons incubated with CXCL10 (Treatment,  $F_{1,54} = 9.342$ ,  $P < 0.01$ ; Current,  $F_{2,54} = 203.2$ ,  $P < 0.0001$ ; Interaction,  $F_{2,54} = 1.165$ ,  $P > 0.05$ , two-way ANOVA, Fig. 3D, E). We further compared the RP and the membrane capacitance

(CM), and found no significant difference after incubation with CXCL9, CXCL10, or CXCL11, compared to PBS ( $P > 0.05$ , Student's *t*-test, Fig. 3F, G). These data suggest that CXCL10, but not CXCL9 or CXCL11 increases the excitability of DRG neurons.

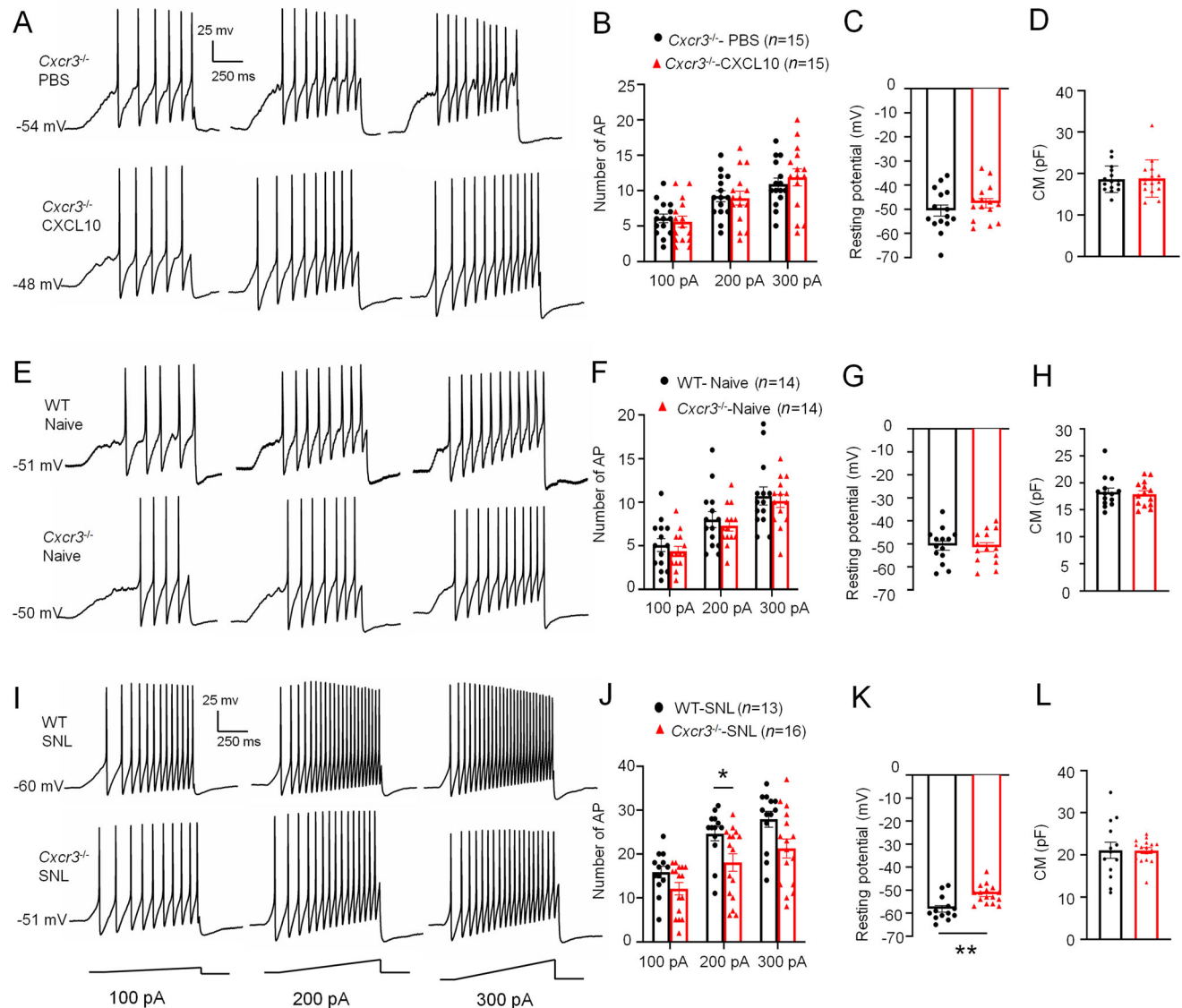


**Fig. 4** The neuronal excitability enhanced by CXCL10 or SNL is decreased in *Cxcr3*<sup>-/-</sup> mice. **A** Examples of membrane potential responses evoked by 1000-ms current injection of 100 pA, 200 pA, and 300 pA in PBS- and CXCL10-treated neurons from *Cxcr3*<sup>-/-</sup> mice. **B** Histogram showing no difference in the numbers of APs in PBS- and CXCL10-treated DRG neurons from *Cxcr3*<sup>-/-</sup> mice (two-way ANOVA). **C, D** No difference in resting potential (**C**) and CM (**D**) between PBS- and CXCL10-treated neurons from *Cxcr3*<sup>-/-</sup> mice (Student's *t*-test). **E** Examples of membrane potential responses evoked by 1000-ms ramp current injection of 100 pA, 200 pA, and 300 pA in neurons from naïve WT and *Cxcr3*<sup>-/-</sup> mice. **F** Histogram showing no difference in the numbers of APs in DRG neurons

between WT mice and *Cxcr3*<sup>-/-</sup> mice (two-way ANOVA). **G, H** Both the resting potential (**G**) and CM (**H**) were comparable in WT and *Cxcr3*<sup>-/-</sup> mice (Student's *t*-test). **I** Examples of membrane potential responses evoked by 1000-ms ramp current injection of 100 pA, 200 pA, and 300 pA in neurons from SNL-treated WT and *Cxcr3*<sup>-/-</sup> mice. **J** Histogram showing a difference in the numbers of APs in DRG neurons between WT and *Cxcr3*<sup>-/-</sup> mice when the injection current is 200 pA (\* $P < 0.05$  vs WT; two-way ANOVA followed by the Bonferroni test). **K** The resting potential of neurons from *Cxcr3*<sup>-/-</sup> mice is significantly higher than that in WT mice (\*\* $P < 0.01$ ; Student's *t*-test). **L** There is no difference between the two groups in CM.

### The Enhanced Excitability of DRG Neurons After CXCL10 Incubation or SNL is Dependent on CXCR3

To check if the increased neuronal excitability induced by CXCL10 is dependent on CXCR3, DRG neurons from *Cxcr3*<sup>-/-</sup> mice were incubated with PBS or CXCL10. In responding to 100 pA, 200 pA, and 300 pA ramp currents, CXCL10 induced numbers of APs similar to PBS in DRG neurons from *Cxcr3*-deficient mice (Treatment,  $F_{1,56} = 0.003$ ,  $P > 0.05$ ; Current,  $F_{2,56} = 132.3$ ,  $P < 0.001$ ; Interaction,  $F_{2,56} = 2.427$ ,  $P > 0.05$ , two-way ANOVA; Fig. 4A, B). In addition, the number of APs induced by CXCL10 in *Cxcr3*<sup>-/-</sup> mice was much smaller than that in WT mice (data shown in Fig. 3E: Treatment,  $F_{1,54} = 8.875$ ,  $P < 0.01$ ; Current,  $F_{2,54} = 268.8$ ,  $P < 0.001$ ; Interaction,  $F_{2,54} = 4.440$ ,  $P < 0.05$ , two-way ANOVA). In *Cxcr3*<sup>-/-</sup> mice, the RP and CM were comparable in the PBS and CXCL10 groups ( $P > 0.05$ , Student's *t*-test; Fig. 4C, D). These data suggest that CXCL10 increases neuronal excitability *via* CXCR3.

The excitability of DRG neurons increases after SNL [27]. To further determine if CXCR3 is involved in this increased excitability, we dissected DRGs from WT and *Cxcr3*<sup>-/-</sup> mice with or without SNL. In naïve mice, there was no significant difference of the AP numbers from WT and *Cxcr3*<sup>-/-</sup> mice (Treatment,  $F_{1,52} = 0.380$ ,  $P > 0.05$ ; Current,  $F_{2,52} = 262.2$ ,  $P < 0.001$ ; Interaction,  $F_{2,52} = 0.055$ ,  $P > 0.05$ , two-way ANOVA; Fig. 4E, F). The RP (Fig. 4G) and CM (Fig. 4H) were also comparable in the two groups. In WT and *Cxcr3*<sup>-/-</sup> mice 7 days after SNL, in responding to 100 pA, 200 pA, and 300 pA ramp current stimulation, the APs of DRG neurons in *Cxcr3*<sup>-/-</sup> mice were significantly fewer than those in WT mice (Treatment,  $F_{1,54} = 5.506$ ,  $P < 0.05$ ; Current,  $F_{2,54} = 126.9$ ,  $P < 0.001$ ; Interaction,  $F_{2,54} = 2.856$ ,  $P < 0.001$ , two-way ANOVA; Fig. 4I, J). The RP of neurons from *Cxcr3*<sup>-/-</sup> mice was significantly higher than that in WT mice ( $P < 0.01$ , Student's *t*-test; Fig. 4K), and there was no significant difference between the two groups in CM ( $P > 0.05$ , Student's *t*-test; Fig. 4L). These results confirm the role of CXCR3 in enhancing neuronal excitability after SNL.

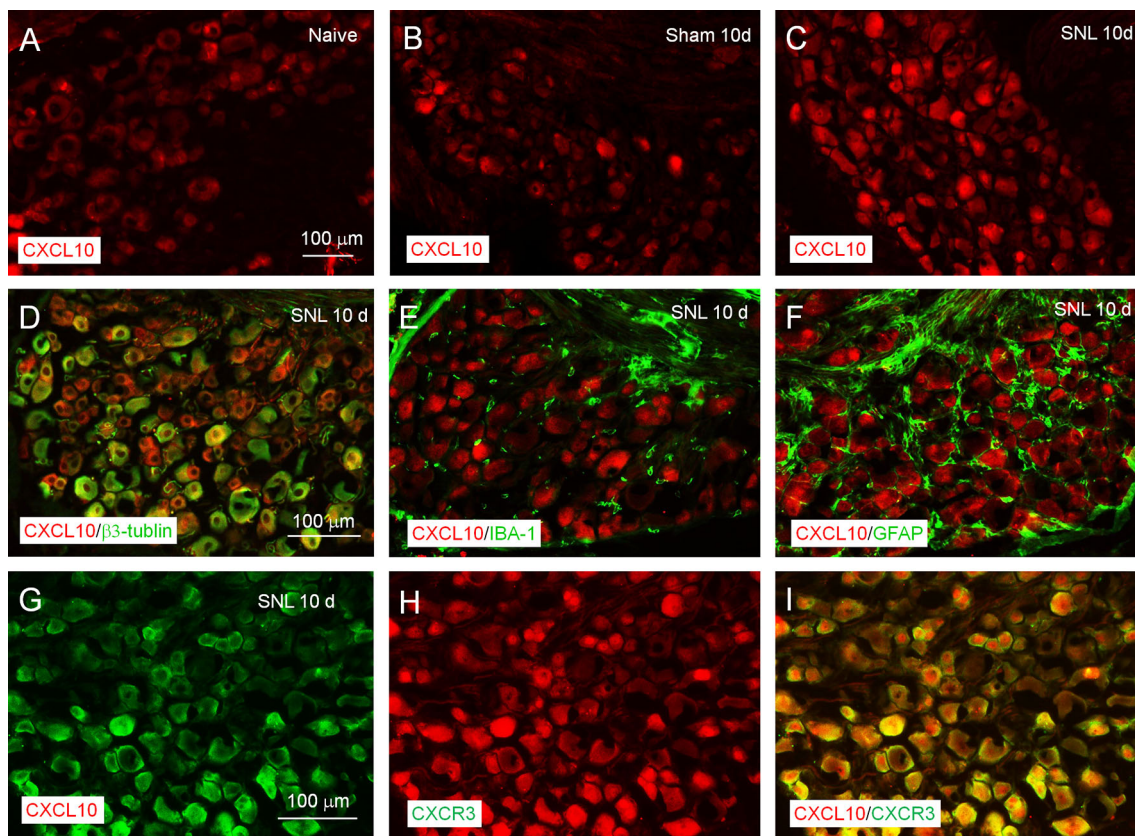


**Fig. 5** SNL increases CXCL10 expression in DRG neurons. **A–C** Fluorescence immunostaining of CXCL10 in the DRG of naïve (**A**), sham (**B**), and SNL (**C**) mice. CXCL10 has low expression in naïve and sham mice, and is increased in SNL mice. **D–F** Double

immunostaining of CXCL10 with β3-tubulin (**D**), IBA-1 (**E**), and GFAP (**F**). CXCL10 is co-localized with β3-tubulin, but not with IBA-1 or GFAP. **G–I** Double staining of CXCL10 (**G**) and CXCR3 (**H**) showing high co-localization (**I**).



## CXCL10 is Expressed in DRG Neurons

As CXCL10 plays a major role in mediating neuronal excitability, we further checked the expression and distribution of CXCL10 by immunostaining. CXCL10-IR was low in the DRGs of naïve (Fig. 5A) and sham-operated mice (Fig. 5B), but was higher in the DRGs of SNL mice (Fig. 5C), confirming the upregulation of CXCL10 after SNL.

To examine CXCL10 distribution in the DRG, we double-stained for CXCL10 with  $\beta$ 3-tubulin, IBA-1, and GFAP. This showed that CXCL10 was co-localized with  $\beta$ 3-tubulin (Fig. 5D), but not with IBA-1 (Fig. 5E) or GFAP (Fig. 5F), indicating the predominant expression of CXCL10 by neurons in the DRG. Furthermore, double-staining of CXCL10 and CXCR3 showed that 94.0% of

CXCL10<sup>+</sup> neurons also expressed CXCR3, and 96.4% of CXCR3<sup>+</sup> neurons expressed CXCL10 (Fig. 5G–I), indicating high co-localization of CXCL10 and CXCR3.

## CXCL10 Induces CXCR3-Dependent p38 and ERK Activation

P38 and ERK are important MAPKs in mediating chronic pain [21]. To determine whether CXCL10 can activate p38 and ERK, we checked the pp38 and pERK expression in ND7/23 cells after incubation with CXCL10 (10 ng/mL). The results showed that pp38 expression was significantly increased after 30 min, 1 h, and 3 h of incubation (30 min, 1.43  $\pm$  0.04-fold,  $P$  < 0.001; 1 h, 1.27  $\pm$  0.08-fold,  $P$  < 0.05; 3 h, 1.23  $\pm$  0.04-fold,  $P$  < 0.05, Student's *t*-test; Fig. 6A, B). pERK expression did not significantly change

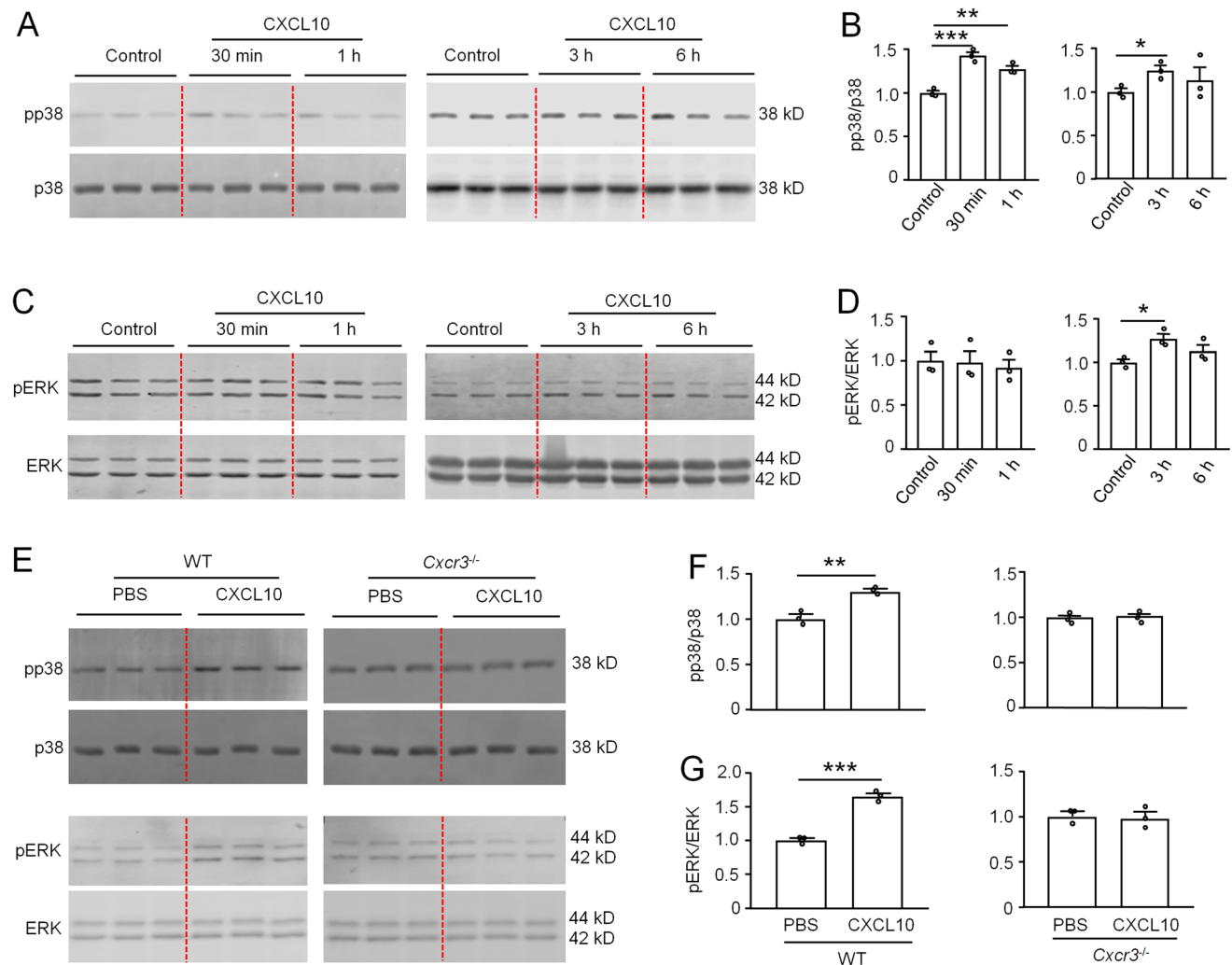


**Fig. 6** CXCL10 increases pERK and P38 activation via CXCR3. **A**, **B** Incubation of CXCL10 (10 ng/mL) increases pp38 expression at 30 min, 1 h, and 6 h ( $n = 3$ /group;  $*P < 0.05$ ,  $***P < 0.001$  vs control group; Student's *t*-test). **C**, **D** Incubation with CXCL10 (10 ng/ml) increases pERK expression at 3 h ( $n = 3$ /group;  $*P < 0.05$  vs control

group; Student's *t*-test). **E**, **F** Intrathecal injection of CXCL10 (100 ng) induces the activation of p38 and ERK in WT mice, but not in *Cxcr3*<sup>-/-</sup> mice ( $n = 3$ /group;  $**P < 0.01$ ,  $***P < 0.001$  vs PBS group; Student's *t*-test).

after 30 min or 1 h, but significantly increased after 3 h of incubation ( $1.28 \pm 0.09$ -fold,  $P < 0.05$ , Student's *t*-test; Fig. 6C, D).

Based on this *in vitro* data, we further checked the pp38 and pERK expression in the DRG 3 h after intrathecal injection of CXCL10 in WT and *Cxcr3*<sup>-/-</sup> mice. As shown in Fig. 6E, CXCL10 induced a significant increase in pp38 expression ( $P < 0.001$ , Student's *t*-test) and pERK expression ( $P < 0.01$ , Student's *t*-test) in WT mice. However, pp38 and pERK expression did not significantly change after CXCL10 injection in *Cxcr3*<sup>-/-</sup> mice ( $P > 0.05$ , Student's *t*-test; Fig. 6E). These results suggest that CXCL10 induces the activation of pERK and pp38 through CXCR3 in DRG neurons.

### P38 Mediates CXCL10-Induced Neuronal Hyperexcitability

As CXCL10 induced rapid (30 min) p38 activation in ND7-23 cells, we asked whether the CXCL10-induced hyperexcitability of DRG neurons (incubation for 30 min) is mediated by p38. We pre-incubated whole-mount DRGs with the p38 MAPK inhibitor SB203580 (10  $\mu\text{mol/L}$ ) [20] for 30 min before CXCL10 treatment. In contrast to vehicle, the number of APs in DRG neurons pretreated with SB203580 was significantly less than neurons treated with CXCL10 only (Treatment,  $F_{1,44} = 25.23$ ,  $P < 0.001$ ; Current,  $F_{2,44} = 274.6$ ,  $P < 0.0001$ ; Interaction,  $F_{2,44} = 4.799$ ,  $P < 0.001$ , two-way ANOVA; Fig. 7 A, B). There was no difference between the two groups in RP ( $P > 0.05$ , Student's *t*-test, Fig. 7C) and CM ( $P > 0.05$ , Student's *t*-test, Fig. 7D). These results suggest that p38 mediates the CXCL10-induced hyperexcitability of DRG neurons.

## Discussion

A growing body of evidence shows that several chemokine receptors are upregulated in the spinal cord and contribute to the pathogenesis of neuropathic pain [2, 5, 7, 8]. However, the role of chemokine receptors in the DRG in neuropathic pain has not been fully investigated. We showed that CXCR3 was persistently increased in DRG neurons after SNL, and specific inhibition of CXCR3 in the DRG attenuated the SNL-induced mechanical allodynia and heat hyperalgesia. In addition, although the three ligands of CXCR3 were upregulated in the DRG after SNL, only CXCL10 increased neuronal excitability in the whole-mount DRG, and this was CXCR3-dependent. In addition, the SNL-induced neuronal hyperexcitability was reduced in *Cxcr3*-deficient mice. We also found that CXCL10 induced CXCR3-dependent activation of p38 and ERK in the DRG. Inhibition of p38-MAPK decreased the

CXCL10-induced hyperexcitability of DRG neurons (Fig. 7E). Thus, our data reveal an important role of CXCL10/CXCR3 in the DRG in regulating neuronal excitability and neuropathic pain.

### Upregulation of CXCR3 in DRG Neurons and the Involvement of CXCR3 in the Pathogenesis of Neuropathic Pain

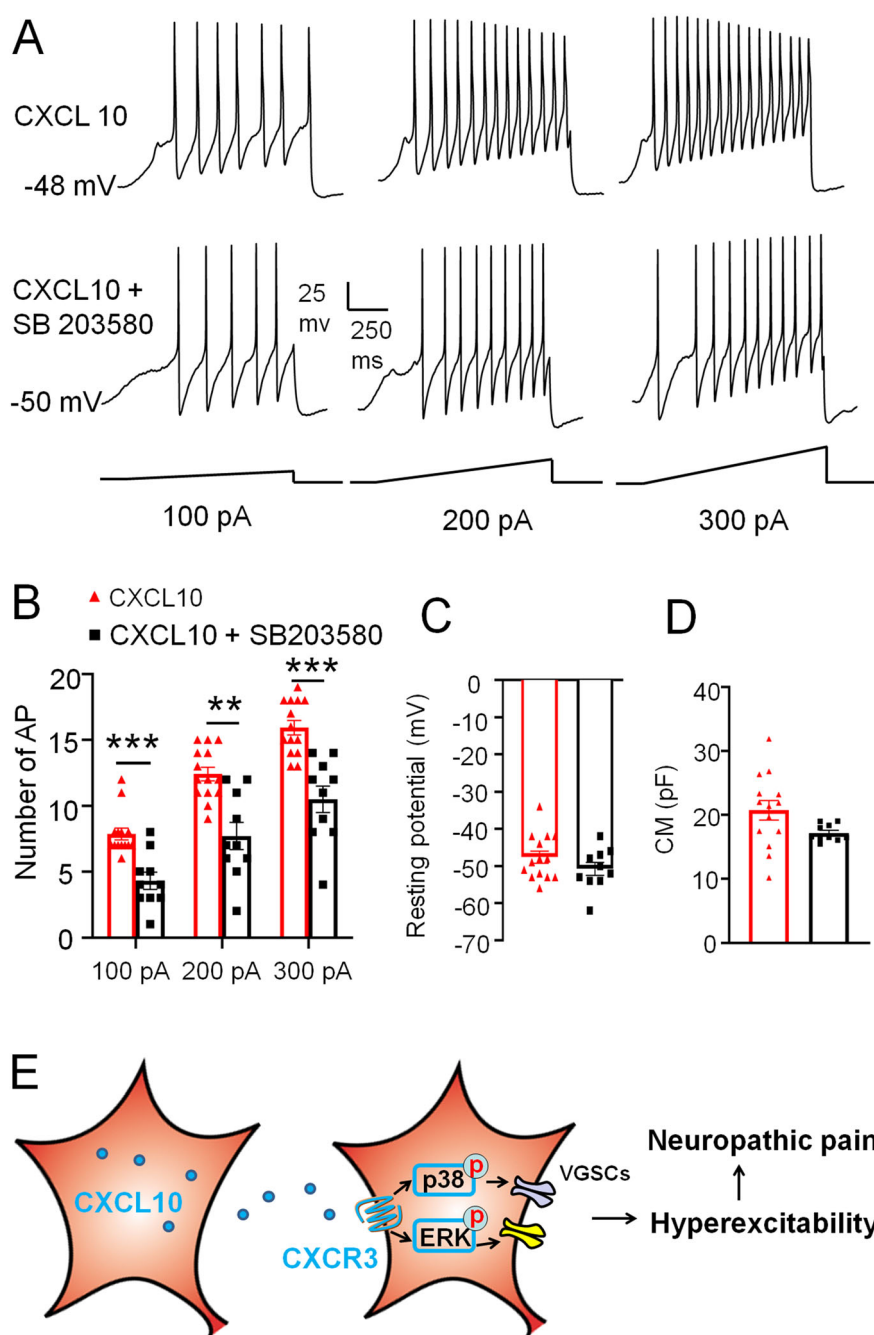
Previous studies have demonstrated that CXCR3 is constitutively expressed in a subpopulation of neurons in the neocortex, hippocampus, striatum, and spinal cord where it plays a vital role in the pathogenesis of a variety of neuroinflammatory and neurodegenerative diseases, including Alzheimer's disease, bipolar disorder, multiple sclerosis, and chronic itch [26, 30–32]. In the spinal cord, CXCR3 expression is increased in neurons, microglia, and astrocytes in animal models of neuropathic pain and cancer pain [7, 12]. Here, we showed that CXCR3 was expressed in DRG neurons and increased after SNL. In agreement with our results, CXCR3 is increased in DRG neurons in the bone cancer pain model in rats and in the chronic constriction injury model in mice [12, 33]. In addition, CXCR3 is distributed in non-peptidergic, peptidergic, and A-type neurons in the DRG [12, 33], suggesting wide expression in all DRG neurons.

We previously reported that *Cxcr3*<sup>-/-</sup> mice show normal basal pain thresholds and motor function [7], but SNL-induced mechanical allodynia and heat hyperalgesia are alleviated from day 3 to day 28 [7]. Intrathecal injection of the CXCR3-specific antagonist NBI-74330 alleviates the chronic pain symptoms induced by SNL, chronic constriction injury, or bone cancer [7, 12, 33]. Intraspinal injection of LV-*Cxcr3* shRNA to specifically inhibit CXCR3 in the spinal cord attenuates the SNL-induced mechanical allodynia and heat hyperalgesia [7], indicating a role of spinal CXCR3 in the maintenance of neuropathic pain. In the present study, we injected LV-*Cxcr3* shRNA into the DRG immediately after the SNL operation. As it usually takes 3–4 days for shRNA to show an effect [5, 6], we started to examine the pain behaviors 5 days after injection. The behavioral data showed that SNL-induced mechanical allodynia and heat hyperalgesia were attenuated from day 5 after SNL and maintained for >14 days, suggesting that CXCR3 in the DRG also plays a role in the maintenance of neuropathic pain.

### CXCL10, but not CXCL9 or CXCL11, Regulates Neuronal Excitability of DRG Sensory Neurons via CXCR3

Hyperexcitability of injured DRG neurons is critical in the development and maintenance of neuropathic pain

**Fig. 7** P38 mediates CXCL10-induced neuronal hyperexcitability. **A** Examples of membrane potential responses evoked by 1000-ms ramp current injection of 100, 200, and 300 pA in neurons treated with SB203580+CXCL10 and CXCL10 only. **B** Histogram showing a significant decrease in the numbers of APs in DRG neurons pretreated with SB203580 compared to CXCL10 only (\*\* $P < 0.01$ , \*\*\* $P < 0.001$ ; two-way ANOVA followed by the Bonferroni test). **C, D** DRG neurons incubated with SB203580+CXCL10 and CXCL10 show no differences in resting potential (**C**) and CM (**D**) (Student's *t*-test). **E** Schematic of the mechanism by which CXCL10/CXCR3 mediates neuropathic pain. SNL increases the expression of CXCL10 and CXCR3 in DRG neurons. CXCL10 is released and acts on CXCR3 to induce the activation of p38 and ERK, which further phosphorylate VGSCs, enhance the excitability of DRG neurons, and contribute to neuropathic pain.



following peripheral nerve injury [34, 35]. Voltage-gated Na<sup>+</sup> channels (VGSCs) are well-known to play critical roles in regulating the excitability of neurons [36]. Nav1.3, Nav1.7, Nav1.8, and Nav1.9 have been demonstrated to be linked to pathological pain by regulating the AP and firing properties of DRG neurons [36]. Accumulating evidence supports the idea that the function of VGSCs can be regulated by inflammatory mediators, such as pro-inflammatory cytokines and chemokines [16]. Recent studies have shown that chemokines including CCL2, CXCL1, and CXCL13 regulate the Na<sup>+</sup> currents of DRG neurons *via*

increasing the expression of Nav1.7 and Nav1.8 or increasing the current density [17, 18, 20, 37]. Accordingly, inhibition or deletion of Nav1.7, Nav1.8, and Nav1.9 attenuates neuropathic pain [38, 39].

In the present study, SNL increased the expression of CXCL9, CXCL10, and CXCL11 with different time-courses. CXCL9 and CXCL11 were only increased in the late phase but CXCL10 was persistently increased after SNL. Surprisingly, incubating DRG neurons with CXCL10 increased their excitability, whereas the same dose of CXCL9 and CXCL11 did not affect the numbers of APs.

Our previous study also found that intrathecal injection of CXCL9 or CXCL11 does not induce pain hypersensitivity in naïve mice [13]. In addition, CXCL10 increases the frequency and amplitude of spontaneous excitatory postsynaptic currents (sEPSCs) [7], and CXCL9 and CXCL11 increase the frequency of both sEPSCs and spontaneous inhibitory PSCs in lamina II neurons [13], suggesting a distinct and presynaptic effect of CXCL9 and CXCL11. It has been reported that CXCL9, CXCL10, and CXCL11 have different binding affinities for CXCR3 [40–42], and activation of CXCR3 by the three ligands requires distinct intracellular domains and causes differences in the downstream responses [43]. Whether the different roles of CXCL9/CXCL11 and CXCL10 in DRG neurons are due to the special intracellular structure of CXCR3 needs to be further investigated. In addition, here we only examined the effect of CXCL9/CXCL10/CXCL11 on the excitability of small-diameter neurons. As CXCR3 is also expressed in large DRG neurons, and these neurons could be sensitized by cell-type switching through over-expression of the hyperpolarization-activated cyclic nucleotide-gated channel (HCN1/2) and COX1 and are important in the maintenance of inflammatory pain [44], it is important to test the roles of the three chemokines in the excitability of large DRG neurons in future studies.

### CXCL10/CXCR3 Activates p38 and ERK MAPKs in the DRG

Microarray assays showed that CXCL10 is one of the highly upregulated chemokines in the spinal cord after SNL [7]. In addition, CXCL10 is constitutively expressed in dorsal horn neurons but induced in astrocytes after SNL and mediates neuropathic pain *via* astrocyte-neuron interaction in the spinal cord [7]. We also found an increase of CXCL10 in the DRG from 3 to 21 days after SNL, a time-course similar to that in the spinal cord [7]. In contrast, CXCL10 is expressed in neurons of the DRG in both naïve and SNL animals. As CXCR3 is also expressed in neurons and CXCL10 and CXCR3 are highly co-localized, CXCL10/CXCR3 signaling may have an autocrine/paracrine function within the DRG. It is noteworthy that the cellular distribution of chemokines and receptors may vary depending on tissues and conditions. For example, CCL2 is expressed in astrocytes in the spinal cord but in neurons in the nucleus accumbens [45] and DRG [46]. In addition, different chemokines and their receptors may have different cellular distributions in the DRG. For example, CXCL12 and its receptor CXCR4 are respectively expressed in satellite glial cells and neurons in the DRG, and participate in the MAPK-mediated up-regulation of ion channels (such as Nav1.8, HCN1/2, and COX1) *via* glial-neuronal interactions [37, 47]. On the contrary, CX3CL1 is

released from DRG neurons and binds to CX3CR1 on satellite cells, resulting in the production of proinflammatory cytokines [48].

The binding of chemokines to their cognate receptors triggers structural rearrangements of the receptor and leads to the activation of intracellular signaling pathways, such as the phospholipase C pathway, the phosphatidylinositol-3 kinase (PI3K) pathway, and the MAPK pathway [4]. Previous studies have demonstrated that CXCR3 can activate several intracellular kinases, such as Ras/ERK, PI3K/AKT, and STAT3 [49, 50]. CXCL10/CXCR3 induced ERK activation in dorsal horn neurons [7]. In ND7-23 neuronal cells, CXCL10 induced a rapid p38 activation a delayed ERK activation. Intrathecal injection of CXCL10 induced the activation of p38 and ERK in WT mice, but not in *Cxcr3*-deficient mice, suggesting that p38 and ERK are downstream of CXCL10/CXCR3. pp38 and Nav1.8 are co-localized in DRG neurons [24], and p38 directly phosphorylates Nav1.8 to increase Nav1.8 current density [25]. Here, we showed that a p38 inhibitor reduced the CXCL10-induced hyperexcitability of DRG neurons, which may also be mediated by regulation of the function of Nav1.8. As the DRG neurons were incubated with CXCL10 for 30 min before electrophysiological recording, but ERK activation was induced 3 h after incubation, we did not examine the effect of an MEK inhibitor on the hyperexcitability induced by CXCL10. Given that CXCL10 was persistently increased in the DRG after SNL, ERK may also be involved in the increased neuronal excitability by directly regulating the function of Nav1.7 [24] or increasing the expression of Na<sup>+</sup> channels [23].

In summary, we explored the role of CXCR3 signaling in the DRG in neuropathic pain. Our results demonstrated that CXCR3 can be activated by CXCL10 and induces downstream p38 and ERK activation, which increases neuronal excitability and further contributes to the maintenance of neuropathic pain. Combined with the important role of CXCL10/CXCR3 in the spinal cord in central sensitization, the CXCL10/CXCR3 pathway may be a promising target for the treatment of neuropathic pain.

**Acknowledgements** This work was supported by the National Natural Science Foundation of China (31871064 and 32030048), the Natural Science Research Program of Jiangsu Province, China (BK20171255), and the Postgraduate Research & Practice Innovation Program of Jiangsu Province, China (KYCX19 2088).

**Conflict of interest** All authors claim that there are no conflicts of interest.

### References

1. Gilron I, Baron R, Jensen T. Neuropathic pain: principles of diagnosis and treatment. *Mayo Clin Proc* 2015, 90: 532–545.

2. Zhang ZJ, Jiang BC, Gao YJ. Chemokines in neuron-glia cell interaction and pathogenesis of neuropathic pain. *Cell Mol Life Sci* 2017, 74: 3275–3291.
3. Xie RG, Gao YJ, Park CK, Lu N, Luo C, Wang WT, *et al.* Spinal CCL2 promotes central sensitization, long-term potentiation, and inflammatory pain *via* CCR2: Further insights into molecular, synaptic, and cellular mechanisms. *Neurosci Bull* 2018, 34: 13–21.
4. Gao YJ, Ji RR. Chemokines, neuronal-glia interactions, and central processing of neuropathic pain. *Pharmacol Ther* 2010, 126: 56–68.
5. Jiang BC, Cao DL, Zhang X, Zhang ZJ, He LN, Li CH, *et al.* CXCL13 drives spinal astrocyte activation and neuropathic pain *via* CXCR5. *J Clin Invest* 2016, 126: 745–761.
6. Zhang ZJ, Cao DL, Zhang X, Ji RR, Gao YJ. Chemokine contribution to neuropathic pain: respective induction of CXCL1 and CXCR2 in spinal cord astrocytes and neurons. *Pain* 2013, 154: 2185–2197.
7. Jiang BC, He LN, Wu XB, Shi H, Zhang WW, Zhang ZJ, *et al.* Promoted interaction of C/EBPalpha with demethylated *Cxcr3* gene promoter contributes to neuropathic pain in mice. *J Neurosci* 2017, 37: 685–700.
8. Gao YJ, Zhang L, Samad OA, Suter MR, Yasuhiko K, Xu ZZ, *et al.* JNK-induced MCP-1 production in spinal cord astrocytes contributes to central sensitization and neuropathic pain. *J Neurosci* 2009, 29: 4096–4108.
9. LINDIA JA, McGOWAN E, JOCHNOWITZ N, ABBADIE C. Induction of CX3CL1 expression in astrocytes and CX3CR1 in microglia in the spinal cord of a rat model of neuropathic pain. *J Pain* 2005, 6: 434–438.
10. Koper OM, Kaminska J, Sawicki K, Kemon H. CXCL9, CXCL10, CXCL11, and their receptor (CXCR3) in neuroinflammation and neurodegeneration. *Adv Clin Exp Med* 2018, 27: 849–856.
11. Tokunaga R, Zhang W, Naseem M, Puccini A, Berger MD, Soni S, *et al.* CXCL9, CXCL10, CXCL11/CXCR3 axis for immune activation - A target for novel cancer therapy. *Cancer Treat Rev* 2018, 63: 40–47.
12. Guan XH, Fu QC, Shi D, Bu HL, Song ZP, Xiong BR, *et al.* Activation of spinal chemokine receptor CXCR3 mediates bone cancer pain through an Akt-ERK crosstalk pathway in rats. *Exp Neurol* 2015, 263: 39–49.
13. Wu XB, He LN, Jiang BC, Shi H, Bai XQ, Zhang WW, *et al.* Spinal CXCL9 and CXCL11 are not involved in neuropathic pain despite an upregulation in the spinal cord following spinal nerve injury. *Mol Pain* 2018, 14: 1744806918777401.
14. Groom JR, Luster AD. CXCR3 ligands: redundant, collaborative and antagonistic functions. *Immunol Cell Biol* 2011, 89: 207–215.
15. Van Raemdonck K, Van den Steen PE, Liekens S, Van Damme J, Struyf S. CXCR3 ligands in disease and therapy. *Cytokine Growth Factor Rev* 2015, 26: 311–327.
16. Miller RJ, Jung H, Bhargoo SK, White FA. Cytokine and chemokine regulation of sensory neuron function. *Handb Exp Pharmacol* 2009: 417–449.
17. Kao DJ, Li AH, Chen JC, Luo RS, Chen YL, Lu JC, *et al.* CC chemokine ligand 2 upregulates the current density and expression of TRPV1 channels and Nav1.8 sodium channels in dorsal root ganglion neurons. *J Neuroinflammation* 2012, 9: 189.
18. Wang JG, Strong JA, Xie W, Yang RH, Coyle DE, Wick DM, *et al.* The chemokine CXCL1/growth related oncogene increases sodium currents and neuronal excitability in small diameter sensory neurons. *Mol Pain* 2008, 4: 38.
19. Yang RH, Strong JA, Zhang JM. NF-kappaB mediated enhancement of potassium currents by the chemokine CXCL1/growth related oncogene in small diameter rat sensory neurons. *Mol Pain* 2009, 5: 26.
20. Wu XB, Cao DL, Zhang X, Jiang BC, Zhao LX, Qian B, *et al.* CXCL13/CXCR5 enhances sodium channel Nav1.8 current density *via* p38 MAP kinase in primary sensory neurons following inflammatory pain. *Sci Rep* 2016, 6: 34836.
21. Ji RR, Gereau RWt, Malcangio M, Strichartz GR. MAP kinase and pain. *Brain Res Rev* 2009, 60: 135–148.
22. Obata K, Noguchi K. MAPK activation in nociceptive neurons and pain hypersensitivity. *Life Sci* 2004, 74: 2643–2653.
23. Zhuang ZY, Xu H, Clapham DE, Ji RR. Phosphatidylinositol 3-kinase activates ERK in primary sensory neurons and mediates inflammatory heat hyperalgesia through TRPV1 sensitization. *J Neurosci* 2004, 24: 8300–8309.
24. Stamboulian S, Choi JS, Ahn HS, Chang YW, Tyrrell L, Black JA, *et al.* ERK1/2 mitogen-activated protein kinase phosphorylates sodium channel Na(v)1.7 and alters its gating properties. *J Neurosci* 2010, 30: 1637–1647.
25. Hudmon A, Choi JS, Tyrrell L, Black JA, Rush AM, Waxman SG, *et al.* Phosphorylation of sodium channel Na(v)1.8 by p38 mitogen-activated protein kinase increases current density in dorsal root ganglion neurons. *J Neurosci* 2008, 28: 3190–3201.
26. Jing PB, Cao DL, Li SS, Zhu M, Bai XQ, Wu XB, *et al.* Chemokine receptor CXCR3 in the spinal cord contributes to chronic itch in mice. *Neurosci Bull* 2018, 34: 54–63.
27. Zhang ZJ, Guo JS, Li SS, Wu XB, Cao DL, Jiang BC, *et al.* TLR8 and its endogenous ligand miR-21 contribute to neuropathic pain in murine DRG. *J Exp Med* 2018, 215: 3019–3037.
28. Dixon WJ. Efficient analysis of experimental observations. *Annu Rev Pharmacol Toxicol* 1980, 20: 441–462.
29. Hargreaves K, Dubner R, Brown F, Flores C, Joris J. A new and sensitive method for measuring thermal nociception in cutaneous hyperalgesia. *Pain* 1988, 32: 77–88.
30. Balashov KE, Rottman JB, Weiner HL, Hancock WW. CCR5(+) and CXCR3(+) T cells are increased in multiple sclerosis and their ligands MIP-1alpha and IP-10 are expressed in demyelinating brain lesions. *Proc Natl Acad Sci U S A* 1999, 96: 6873–6878.
31. Xia MQ, Bacskai BJ, Knowles RB, Qin SX, Hyman BT. Expression of the chemokine receptor CXCR3 on neurons and the elevated expression of its ligand IP-10 in reactive astrocytes: in vitro ERK1/2 activation and role in Alzheimer's disease. *J Neuroimmunol* 2000, 108: 227–235.
32. Israelsson C, Bengtsson H, Lobell A, Nilsson LN, Kylberg A, Isaksson M, *et al.* Appearance of Cxcl10-expressing cell clusters is common for traumatic brain injury and neurodegenerative disorders. *Eur J Neurosci* 2010, 31: 852–863.
33. Chen Y, Yin D, Fan B, Zhu X, Chen Q, Li Y, *et al.* Chemokine CXCL10/CXCR3 signaling contributes to neuropathic pain in spinal cord and dorsal root ganglia after chronic constriction injury in rats. *Neurosci Lett* 2019, 694: 20–28.
34. Devor M. Ectopic discharge in Abeta afferents as a source of neuropathic pain. *Exp Brain Res* 2009, 196: 115–128.
35. Govrin-Lippmann R, Devor M. Ongoing activity in severed nerves: Source and variation with time. *Brain Res* 1978, 159: 406–410.
36. Dib-Hajj SD, Cummins TR, Black JA, Waxman SG. Sodium channels in normal and pathological pain. *Annu Rev Neurosci* 2010, 33: 325–347.
37. Yang F, Sun W, Yang Y, Wang Y, Li CL, Fu H, *et al.* SDF1-CXCR4 signaling contributes to persistent pain and hypersensitivity *via* regulating excitability of primary nociceptive neurons: involvement of ERK-dependent Nav1.8 up-regulation. *J Neuroinflammation* 2015, 12: 219.
38. Luiz AP, Wood JN. Sodium Channels in Pain and Cancer: New Therapeutic Opportunities. *Adv Pharmacol* 2016, 75: 153–178.

39. Bang S, Yoo J, Gong X, Liu D, Han Q, Luo X, *et al.* Differential inhibition of Nav1.7 and neuropathic pain by hybridoma-produced and recombinant monoclonal antibodies that target Nav1.7: Differential activities of Nav1.7-targeting monoclonal antibodies. *Neurosci Bull* 2018, 34: 22–41.
40. Cole KE, Strick CA, Paradis TJ, Ogborne KT, Loetscher M, Gladue RP, *et al.* Interferon-inducible T cell alpha chemoattractant (I-TAC): A novel non-ELR CXC chemokine with potent activity on activated T cells through selective high affinity binding to CXCR3. *J Exp Med* 1998, 187: 2009–2021.
41. Cox MA, Jenh CH, Gonsiorek W, Fine J, Narula SK, Zavodny PJ, *et al.* Human interferon-inducible 10-kDa protein and human interferon-inducible T cell alpha chemoattractant are allotropic ligands for human CXCR3: Differential binding to receptor states. *Mol Pharmacol* 2001, 59: 707–715.
42. Weng Y, Siciliano SJ, Waldburger KE, Sirotina-Meisher A, Staruch MJ, Daugherty BL, *et al.* Binding and functional properties of recombinant and endogenous CXCR3 chemokine receptors. *J Biol Chem* 1998, 273: 18288–18291.
43. Colvin RA, Campanella GS, Sun J, Luster AD. Intracellular domains of CXCR3 that mediate CXCL9, CXCL10, and CXCL11 function. *J Biol Chem* 2004, 279: 30219–30227.
44. Sun W, Yang F, Wang Y, Fu H, Yang Y, Li CL, *et al.* Contribution of large-sized primary sensory neuronal sensitization to mechanical allodynia by upregulation of hyperpolarization-activated cyclic nucleotide gated channels *via* cyclooxygenase 1 cascade. *Neuropharmacology* 2017, 113: 217–230.
45. Wu XB, Jing PB, Zhang ZJ, Cao DL, Gao MH, Jiang BC, *et al.* Chemokine receptor CCR2 contributes to neuropathic pain and the associated depression via increasing NR2B-mediated currents in both D1 and D2 dopamine receptor-containing medium spiny neurons in the nucleus accumbens shell. *Neuropsychopharmacology* 2018, 43: 2320–2330.
46. Zhu X, Cao S, Zhu MD, Liu JQ, Chen JJ, Gao YJ. Contribution of chemokine CCL2/CCR2 signaling in the dorsal root ganglion and spinal cord to the maintenance of neuropathic pain in a rat model of lumbar disc herniation. *J Pain* 2014, 15: 516–526.
47. Yang F, Sun W, Luo WJ, Yang Y, Yang F, Wang XL, *et al.* SDF1-CXCR4 signaling contributes to the transition from acute to chronic pain state. *Mol Neurobiol* 2017, 54: 2763–2775.
48. Souza GR, Talbot J, Lotufo CM, Cunha FQ, Cunha TM, Ferreira SH. Fractalkine mediates inflammatory pain through activation of satellite glial cells. *Proc Natl Acad Sci U S A* 2013, 110: 11193–11198.
49. Zhang C, Li Z, Xu L, Che X, Wen T, Fan Y, *et al.* CXCL9/10/11, a regulator of PD-L1 expression in gastric cancer. *BMC Cancer* 2018, 18: 462.
50. Bonacchi A, Romagnani P, Romanelli RG, Efsen E, Annunziato F, Lasagni L, *et al.* Signal transduction by the chemokine receptor CXCR3: activation of Ras/ERK, Src, and phosphatidylinositol 3-kinase/Akt controls cell migration and proliferation in human vascular pericytes. *J Biol Chem* 2001, 276: 9945–9954.